

Supporting information for the manuscript

Spin-coated films of gadolinium formate for cryogenic cooling

Inés Tejedor,^a María Isabel Calvo,^a Jesús Gandara-Loe,^b Víctor Rubio-Giménez,^b Rob Ameloot,^b Ignacio Gascón,^a and Olivier Roubeau^{a,*}

^a Instituto de Nanociencia y Materiales de Aragón (INMA), CSIC and Universidad de Zaragoza, Zaragoza 50009, Spain. E-mail: roubeau@unizar.es.

^b Centre for Membrane Separation, Adsorption, Catalysis and Spectroscopy, KU Leuven, Celestijnenlaan 200F, Leuven 3001, Belgium. E-mail: rob.ameloot@kuleuven.be.

Table of contents

<i>Physical characterization</i>	p. S2
Scheme S1. Set-up used for heat capacity measurements	p. S3
<i>Reagents, substrates and synthesis of Gd(HCOO)₃ particles</i>	p. S4
<i>Attempts of spin-coating aqueous solutions of Gd(HCOO)₃</i>	p. S5
Figure S1. SEM observations of spin-coating aqueous Gd(HCOO) ₃ on Si	p. S5
Figure S2. SEM observations of Gd(HCOO) ₃ particles	p. S6
Figure S3. Characterization of Gd(HCOO) ₃ particles	p. S7
<i>Attempts of spin-coating dispersions of pre-formed Gd(HCOO)₃</i>	p. S8
Figure S4. DLS of MeOH and 1:5 MeOH:CHCl ₃ dispersions Gd(HCOO) ₃ particles	p. S8
Figure S5. Optical images of spin-coating attempts with a MeOH dispersion	p. S9
<i>Attempts at making Langmuir-Blodgett films of Gd(HCOO)₃ particles</i>	p. S10
Figure S6. Pressure-area isotherm and BAM images for Gd(HCOO) ₃ particles	p. S11
Figure S7. SEM observations of LB transfers on Si at 20 mN/m and 40 mN/m	p. S12
Figure S8. DLS of dispersion of Gd(HCOO) ₃ particles coated with oleic acid	p. S12
Figure S9. Pressure-area isotherm and BAM images for Gd(HCOO) ₃ particles coated with oleic acid	p. S13
Figure S10. SEM of LB film of Gd(HCOO) ₃ particles coated with oleic acid	p. S13
<i>Study of bulk reaction of Gd₂O₃ and formic acid vapors</i>	p. S14
Figure S11. PXRD patterns of Gd ₂ O ₃ powder reacted with formic acid vapors	p. S15
<i>Spin-coating of Gd₂O₃ dispersions</i>	p. S15
Figure S12. DLS of Gd ₂ O ₃ dispersions in iso-propanol	p. S15
Figure S13. SEM observation of starting “nano”-powder	p. S15
Figure S14. Optical images of initial attempts of spin-coating	p. S16
Figure S15. SEM images of spin-coated films of Gd ₂ O ₃	p. S16
<i>Transformation of Gd₂O₃ films into Gd(HCOO)₃</i>	p. S17
Figure S16. GIXRD and SEM observations before and after reaction	p. S17
Figure S17. Magnetic characterization before and after reaction	p. S17
<i>Reaction of Gd₂O₃ in formic acid at RT</i>	p. S18
Figure S18. PXRD of the reaction products	p. S18
Figure S18. SEM of the reaction products and of the starting Gd ₂ O ₃ powders	p. S19
<i>Spin-coating with formic acid dispersions of Gd(HCOO)₃</i>	p. S20
Figure S20. DLS of formic acid dispersions of Gd(HCOO) ₃	p. S20
Figure S21. SEM images of spin-coated films and particle size distribution	p. S20
Figure S22. SEM images of spin-coated films at various flux	p. S21
Figure S23. SEM images of spin-coated films at various velocities and times	p. S22
Table S1. Estimation of the mass of spin-coated Gd(HCOO) ₃	p. S23
Figure S24. Transverse SEM image of spin-coated film at 50°C.	p. S23
Figure S25. Magnetic characterization of a spin-coated film of Gd(HCOO) ₃	p. S24
Figure S26. Temperature dependence of ΔS _m expressed in J K ⁻¹ kg ⁻¹	p. S24
Figure S27. Temperature dependence of S _m	p. S25
Figure S28: Parameters of 2-tau determination of the heat capacity	p. S26

Physical characterization

Powder X-ray diffraction data were obtained at ambient temperature using a Rigaku D-Max diffractometer equipped with a rotating anode and a graphite monochromator to select the Cu-K α wavelength, through the Servicio General de Apoyo a la Investigación-SAI, Universidad de Zaragoza.

Grazing-incidence X-ray diffraction (GIXRD) patterns were recorded using a Malvern PANalytical Empyrean diffractometer over a 4-50° 2 θ range with an incident beam angle of 0.2°. A PIXcel3D solid state detector and a Cu anode (with Cu K α 1 = 1.5406 Å and Cu K α 2 = 1.5444 Å wavelengths) operating at 45 kV and 40 mA were used for all measurements. Thin film samples were placed on a flat stage and measured in scanning line mode with a step size of 0.053° and a counting time of 1000 s per step. On the incident beam side, a 1/32° fixed anti-scatter slit was used to limit the divergence of the beam. Additionally, a 1/8° divergence slit and a 4 mm beam mask were used. At the secondary side, a 1/8° anti-scatter slit together with a 0.04 Soller slit were used.

Infra-red spectra were acquired with either a Varian 670 FT-IR spectrometer (KU Leuven) equipped with an MCT detector (KU Leuven) or a FTIR Bruker Vertex 70 spectrometer (INMA, University of Zaragoza).

Raman spectra were obtained with a WITec Alpha 300 equipped with a confocal microscope (INMA, University of Zaragoza). The laser used was 532 nm. Measurements were made with 25 accumulations, 3 seconds of integration time and a voltage of 1.035 mV.

Scanning Electron Microscopy observations were made by using either a Philips/FEI XL-30 FEG instrument (KU Leuven) or an INSPECT-F50 instrument (LMA, INMA, University of Zaragoza), both operating at an accelerating voltage of 10 keV. Samples were previously sputter-coated with either 2 nm of Pt or 14 nm of Pd.

Dynamic Light Scattering (DLS) experiments were conducted using a Malvern Zetasizer Nano ZS ZEN3600 equipped with a 633 nm laser and configured in a back-scattering arrangement at 173°. Measurements were done at 25°C. The polydispersity index (PDI) calculated by the Malvern software is defined as:

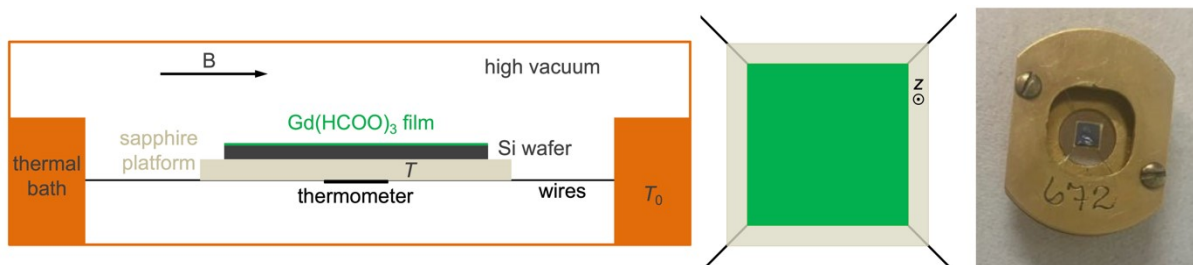
$$PDI = \frac{\sigma^2}{D_z^2}$$

where σ is the standard deviation of the mean diameter size D_z . PDI is dimensionless with values between 0 and 1, which is scaled such that values with 0.10 or less are considered highly monodisperse and values smaller than 0.05 are rarely seen.¹

Magnetic measurements were done with a Quantum Design MPMS XL magnetometer hosted by the Servicio de apoyo a la Investigación – SAI Universidad de Zaragoza. Magnetization vs. temperature (M vs. T , from 2 to 30 K, at 0.1 or 0.5 T) and Magnetization vs. Field (M vs. B , from 0 to 5 T, at 2-10 K) measurements were done, for both pristine 325 μ m thick Si and 325 μ m thick Si covered with spin-coated Gd(HCOO)₃ films. Measurements were performed with samples of 0.3 cm².

¹ Dynamic Light Scattering Common Terms Defined, Malvern Instruments Inform White Paper; 2011. Available at: <http://www.malvern.com/en/support/resource-center/Whitepapers/WP111214DLSTermsDefined.aspx>

Heat capacity measurements were made with the ^3He heat capacity option of a Quantum Design 9 T Physical Properties Measurement System hosted by the Servicio de apoyo a la Investigación – SAI Universidad de Zaragoza. Experiments were done on 0.0625 cm^2 pieces of $325\text{ }\mu\text{m}$ thick Si, either pristine or covered with spin-coated $\text{Gd}(\text{HCOO})_3$ films. The sample was fixed to the sapphire sample holder with little Apiezon N grease (see Scheme S1). Measurements use the relaxation method,² and were made down to 0.38 K in zero-field and at 1 T , 3 T and 5 T applied magnetic field.



Scheme S1. Set-up used for heat capacity measurements: side (left) and top (centre) schematic views, optical picture (right). The raw data are obtained for the platform+sample entity and are corrected by an addenda previously determined.

² a) see quantum Design application note at <https://qd-uki.co.uk/wp-content/uploads/2019/07/Heat-Capacity-and-Helium-3-Application-Note.pdf>, retrieved on 12/06/024; b) for the application of the two-tau model to determine heat capacity from relaxation data, see J. S. Hwang, K. Lin, C. Tien, *Rev. Sci. Instrum.* **1997**, 68, 94

Experimental details

Reagents

HCOOH (ChemLab CAS:64-18-6), Gadolinium (III) oxide (nanopowder, 99.99+% REO), Thermo Scientific Chemicals, CAS: 12064-62-9), Gadolinium (III) oxide (powder, 99.9%, Aldrich, CAS: 12064-62-9), Sulfuric acid (95-97%, Supelco, CAS:7664-93-9) and Hydrogen peroxide (35%, ChemLab. 7722-84-1). Ultra-pure Milli Q water, resistivity 18.2 M Ω ·cm

Substrates

Si wafers with 325 μ m thickness oriented along <100> axis were used. All were cleaned by a piranha solution.

CAUTION: Piranha solutions are extremely corrosive to organic substances and may irritate the respiratory tract if vapor is inadvertently inhaled. Piranha solutions are extremely energetic and may result in explosion or injury if not handled with extreme caution.

Spin-coating

Experiments were done with a spin-coater model Fr10KPA, either at RT (22°C) or at 50°C, using velocities from 1000 to 6000 RPM. Except for initial tests of static spin-coating, all experiments were made in dynamical conditions, i.e. with the substrate spinning before casting the first drop of solution/dispersion. The solutions/dispersions were cast on the spinning substrate at constant flux using a syringe pump. The substrates were in most cases 2 x 2 cm² pieces of Si wafers.

Synthesis of Gd(HCOO)₃

Bulk crystalline powder of Gd(HCOO)₃ was obtained by reaction of Gd₂O₃ powder in pure formic acid (1:30 equivalents) at 80°C for 3 hours. The same synthesis was also performed with increasing amounts of acetic acid (10, 20 and 33% in wt.), in an attempt to modulate the particle size and homogeneity. The solids were recovered and dried in air. No significant effect of the added acetic acid on the particle size was noticed (see Fig. S1).

Purity was checked by PXRD (Fig. S2).

Attempts of spin-coating aqueous solutions of $\text{Gd}(\text{HCOO})_3$

The solubility of $\text{Gd}(\text{HCOO})_3$ in miliQ water was estimated to be ca. 11-12 g/mL. A clear 5 mg/mL solution was prepared and used for initial attempts of direct spin-coating of $\text{Gd}(\text{HCOO})_3$ from its solution. These were done on cut pieces of a 525 mm Si(100) wafer, of ca. 1.2x1.5 cm² sizes.

Static spin-coating was attempted under two conditions:

- 1) 0.5 mL of the solution was cast at the centre of the substrate, while still, after which the substrate was spin at 1000 RPM for 30s, with an initial acceleration of 550 RPM.
- 2) 1.0 mL of the solution was cast at the centre of the substrate, while still, after which the substrate was spin at 200 RPM for 3 min, with an initial acceleration of 110 RPM, and a further 3 min at 500 RPM, with an acceleration of 220 RPM.

Dynamic spin-coating was attempted under two conditions:

- 3) 5.0 mL of the solution was cast drop by drop over 4 min at the centre of the substrate, while spinning at 500 RPM, after which further spinning at 500 RPM (30 s), 1000 RPM (1 min) and 3000 RPM (30 s) was done.
- 4) 6.0 mL of the solution was cast drop by drop over 3 min at the centre of the substrate, while spinning at 500 RPM, after which further spinning at 500 RPM (90 s), 1000 RPM (1min) and 3000 RPM (1 min) was done.

In all cases, there was visually no material left on the substrate, which was confirmed by SEM observations where only some areas showed very little amount of material (Fig. S1a and b).

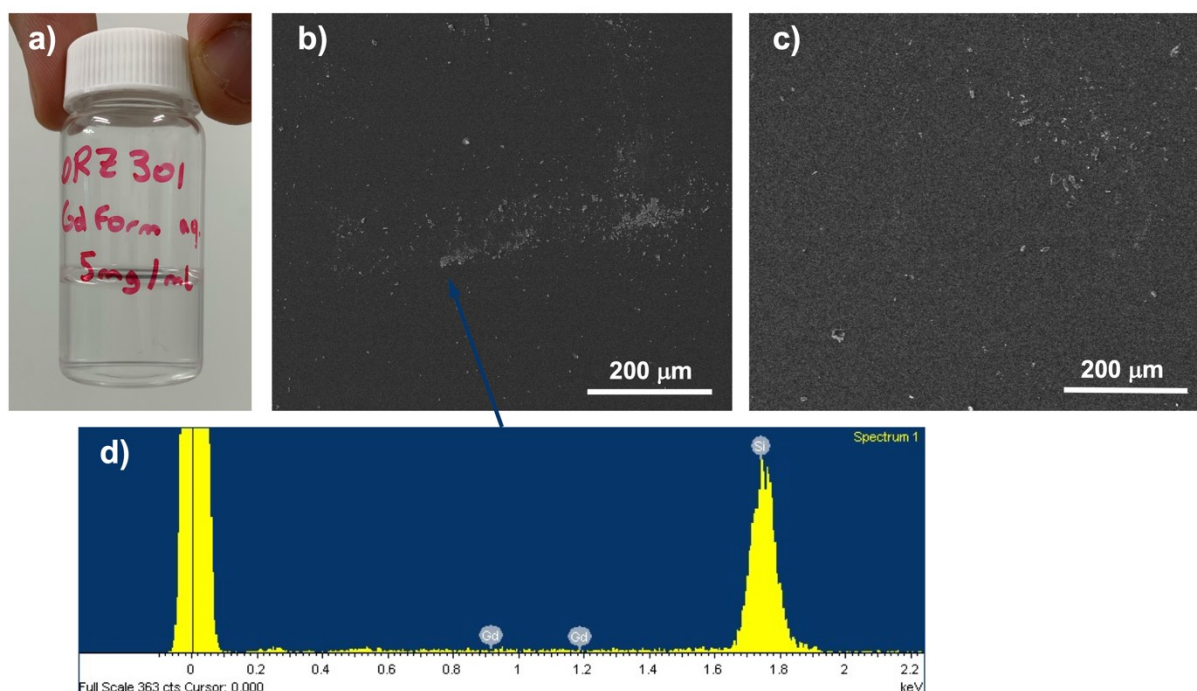


Figure S1. a) 5 mg/mL aqueous solution of $\text{Gd}(\text{HCOO})_3$ used in spin-coating attempts. b) and c) characteristic SEM observations of static (b) and dynamic (c) spin-coating on Si. d) EDX results for a small area in b) with some material deposited, showing no detection of Gd.

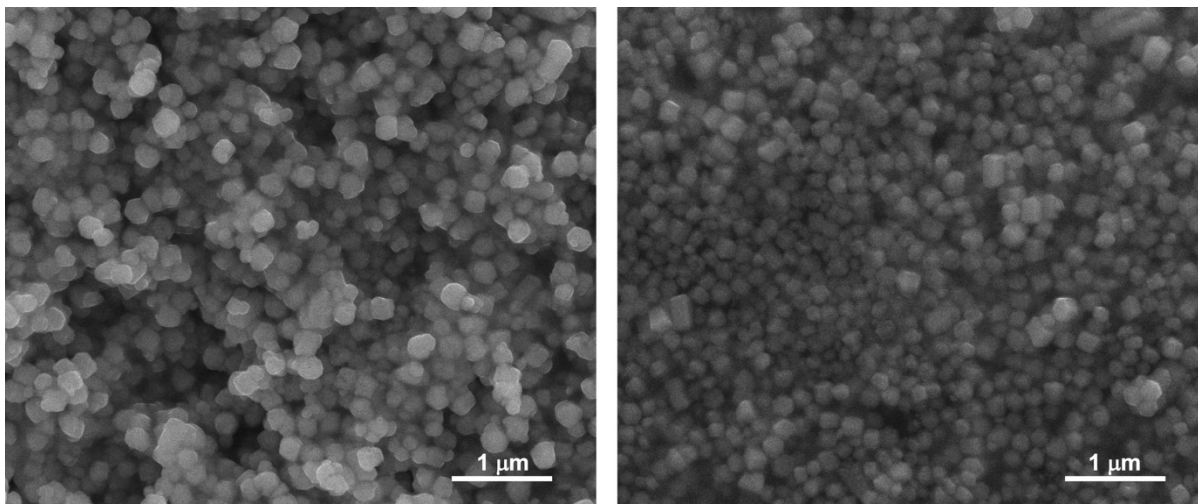


Figure S2. Representative SEM image of $\text{Gd}(\text{HCOO})_3$ obtained by reacting Gd_2O_3 in pure formic acid (1:30 equivalents) at 80°C for 3 hours without (left) and with (right) acetic acid as modulator (33% in wt.). Analysis of size distribution gives respectively 231(31) nm and 219(45) nm.

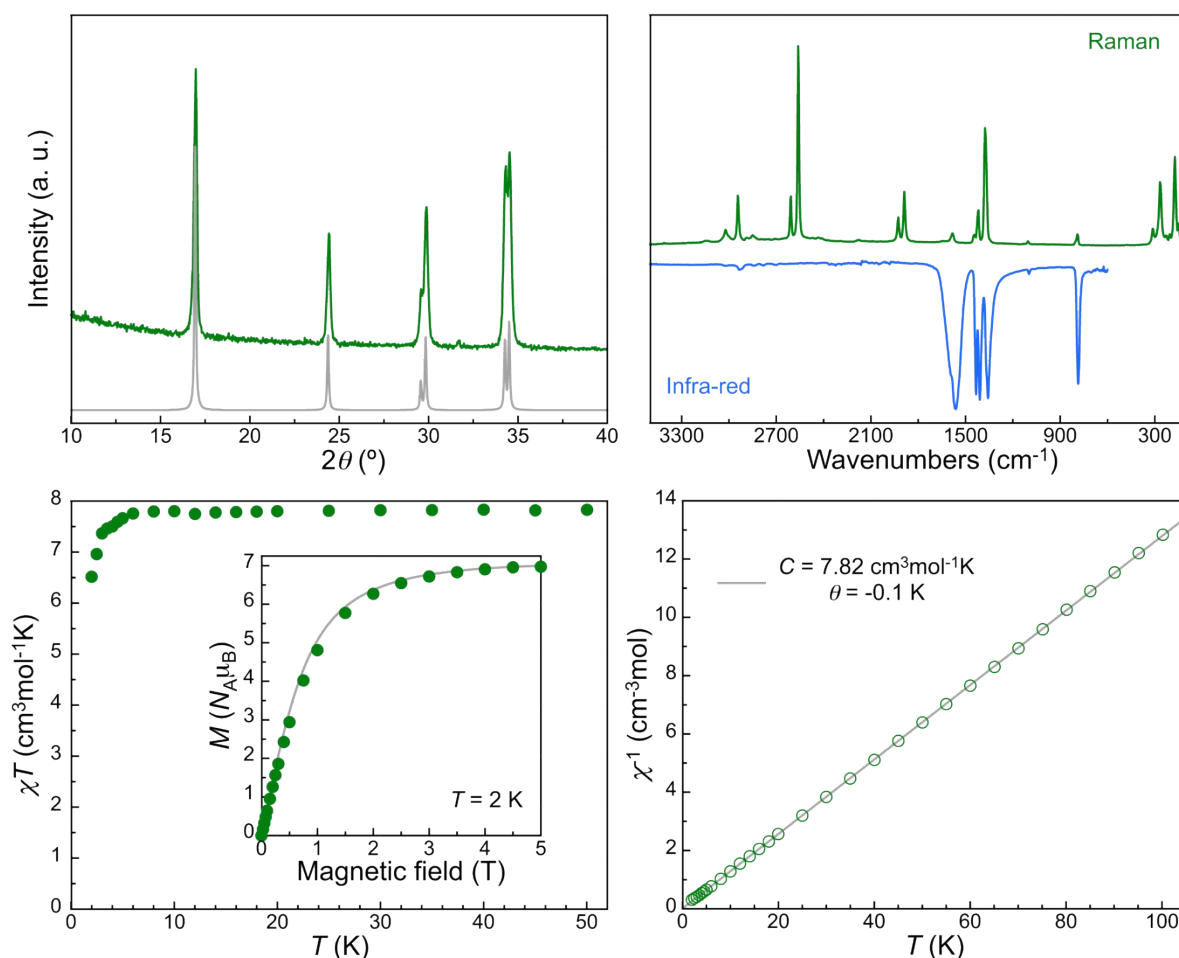


Figure S3. Characterization of $\text{Gd}(\text{HCOO})_3$ obtained by reacting Gd_2O_3 in pure formic acid. Top, left: Powder X-ray diffractogram (green line) compared with the calculated patterns based on the reported single-crystal structure (grey line). Top, right: Raman and Infra-red spectra. Bottom, left: Temperature dependence of the χT product, χ being the molar magnetic susceptibility. Inset: magnetization vs. field at $T = 2$ K, compared with the Brillouin function for a $S = 7/2$ spin and $g = 2.02$ (grey line). Bottom, right: temperature dependence of the inverse magnetic susceptibility χ^{-1} . The grey line is a fit to the Curie-Weiss law, yielding a Curie constant of $7.82 \text{ cm}^3\text{mol}^{-1}\text{K}$ and a Weiss temperature θ of -0.1 K, indicating weak antiferromagnetic interactions, and in excellent agreement with the literature.³

³ G. Lorusso, J. W. Sharples, E. Palacios, O. Roubeau, E. K. Brechin, R. Sessoli, A. Rossin, F. Tuna, E. J. L. McInnes, D. Collison and M. Evangelisti, *Adv. Mater.*, 2013, **25**, 4653

Attempts of spin-coating dispersions of pre-formed $\text{Gd}(\text{HCOO})_3$

Dispersions of the bulk $\text{Gd}(\text{HCOO})_3$ particles obtained above were prepared at 0.25 mg/mL in MeOH, CHCl_3 , and CH_2Cl_2 by applying a 15 min bath ultrasonication. Dynamic Light Scattering measurements showed the latter two were neither stable nor homogeneous.

The MeOH dispersions were relatively stable and showed an average hydrodynamic size in good agreement with SEM observations at 265(94) nm, as well as a good polydispersity index at 0.12 (Fig. S3). Dispersions with higher concentrations up to 2.5 mg/mL can be obtained by increasing the sonication time and show similar DLS results (PDI < 0.2, sizes around 270 nm).

Once prepared, the MeOH dispersions could be diluted with CHCl_3 in a 1:5 proportion without losing stability nor homogeneity (Fig. S3).

Dynamic spin-coating of a 0.5 mg/mL MeOH dispersion on pieces of Si wafers was attempted at RT and various speeds and fluxes. Visually, there was no material deposited (Fig. S4).

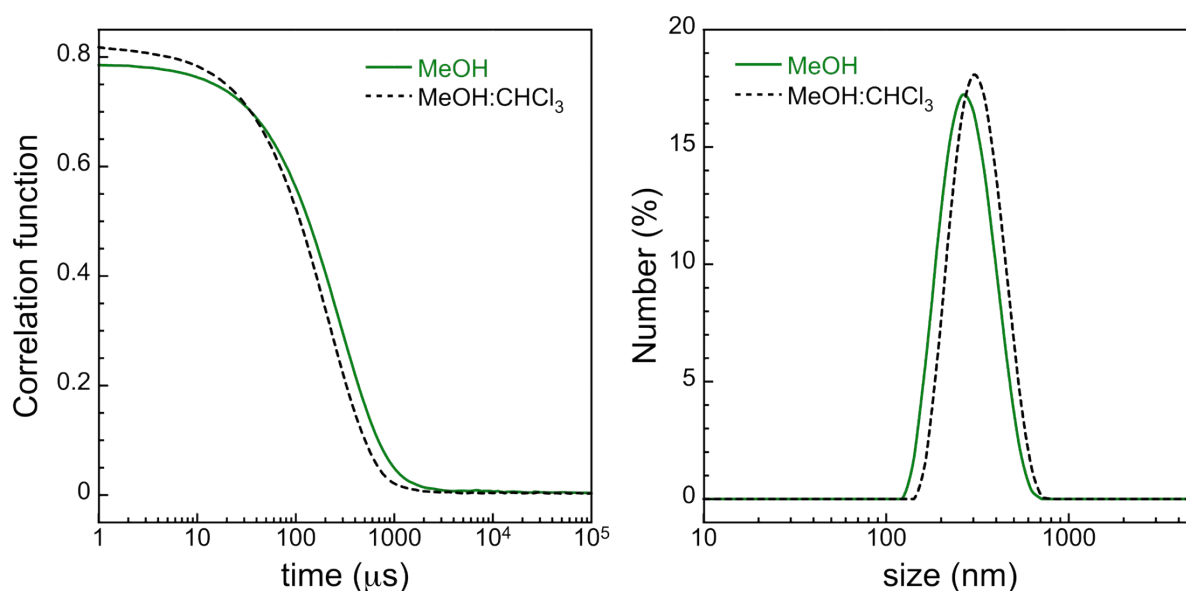


Figure S4. Dynamic Light Scattering of 0.25 mg/mL MeOH (green lines) and 1:5 MeOH:CHCl₃ (dashed black lines) dispersions $\text{Gd}(\text{HCOO})_3$ particles: correlation function vs. time (left) and hydrodynamic size distribution (right).

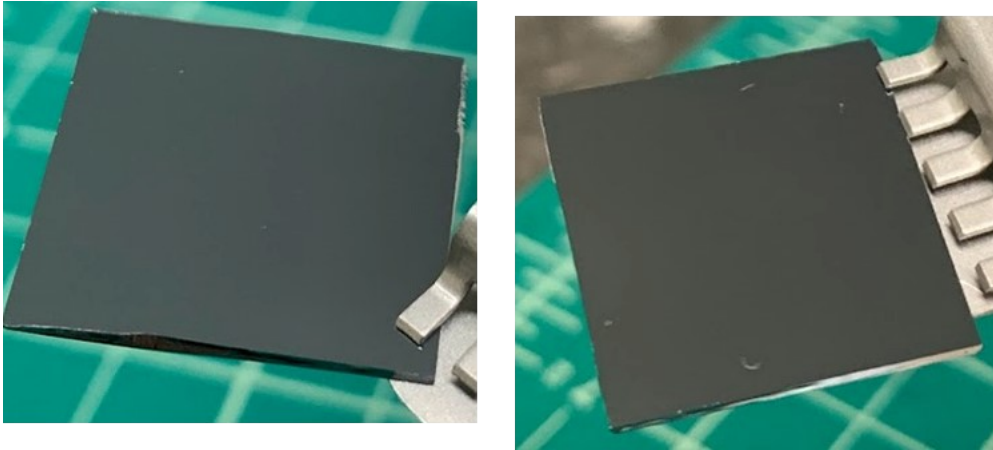


Figure S5. Optical images of spin-coating attempts with a 0.5 mg/mL MeOH dispersion at 4000 and 0.5 mL/min flux (left) and 6000 RPM and 0.25 mL/min flux (right). No material appeared to remain on the Si substrate. The Si pieces are 20×20 mm².

Attempts at making Langmuir-Blodgett films of Gd(HCOO)₃ particles

Since good dispersions can be obtained in MeOH:CHCl₃ 1:5 mixtures, the use of Langmuir-Blodgett technique to form films of Gd(HCOO)₃ was investigated.

Surface pressure–area (π -A) isotherms were obtained using a Teflon Langmuir trough NIMA model 702 (dimensions 720 mm×100 mm). Brewster Angle Microscopy (BAM) images were acquired using a KSV NIMA Micro BAM equipped with a red laser (659 nm, 50 mW) as the light source. The incidence angle was fixed at 53.1°, and a black quartz plate was placed inside the trough as a light trap. The optics of the system provided a spatial resolution of 6 μm per pixel in the water surface plane and a field of view of 3600×4000 μm^2 .

In a typical experiment, the dispersion was carefully spread drop-by-drop using a Hamilton microsyringe onto the aqueous subphase. After letting the solvent evaporate for 20 minutes, compression was performed by a symmetric double-barrier system at a constant speed of 8 $\text{cm}^2\cdot\text{min}^{-1}$. Surface pressure was continuously monitored during the experiments by means of a Wilhelmy balance using a filter paper plate.

Langmuir-Blodgett films were made with a KSV-NIMA trough model 2000-System 3, with dimensions of 775 mm × 120 mm², by vertical-dipping, the substrate being raised at 1 $\text{mm}\cdot\text{min}^{-1}$.

Various combinations of concentrations and expanded volumes were tested, the optimal being expanding 3 mL of a 0.25 mg/mL dispersion. The resulting surface pressure-area isotherm exhibits a gradual increase and a change of slope at ca. 31 mN/m, which could indicate a reorganization of the material at the interface. BAM observations show that the surface seems to be fully covered with material after this change of slope (Fig. S5).

Transfer of the film formed was performed below (20 mN/m) and above (40 mN/m) the change of slope. SEM observations unfortunately show there is no material transferred, at both pressures (Fig. S6). A plausible explanation is that the material forming the film readily dissolves in the aqueous subphase upon immersion of the substrate. Poor wettability of the substrate and poor adhesion of Gd(HCOO)₃ particles may also be involved.

Due to the high solubility of Gd(HCOO)₃ in water, the use of surfactants was attempted. Good dispersions could be made using 3% oleic acid. The change of sign in Z potential and increase in absolute values upon addition of oleic acid indicate the particles are a priori covered with the surfactant and the dispersion is more stable (Fig. S7).

The surface pressure-area isotherm of the resulting dispersion is much more expanded than that without oleic acid and BAM observation seems to point at a more compact and dense film at 32 mN/m (Fig. S8). This denser film was transferred vertically to a Si substrate at 40 mN/m. Although in this case some particles of Gd(HCOO)₃ can be observed through SEM, the resulting film is very inhomogeneous and discontinuous (Fig. S9).

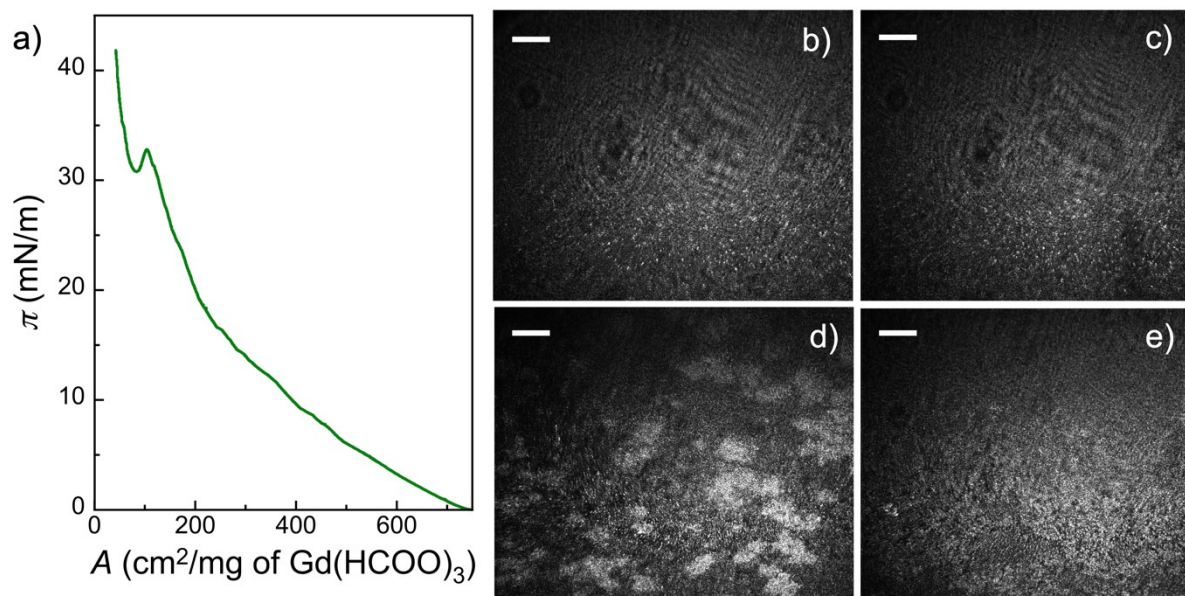


Figure S6. a) Surface pressure-area isotherm for a 0.25 mg/mL dispersion of $\text{Gd}(\text{HCOO})_3$ in $\text{MeOH}:\text{CHCl}_3$ 1:5. b-e) BAM images taken at, respectively, $\pi = 2.5$ mN/m ($A = 921$ cm^2/mg), $\pi = 19.0$ mN/m ($A = 485$ cm^2/mg), $\pi = 32$ mN/m ($A = 65$ cm^2/mg) and change of slope. The scale bar is 500 μm .

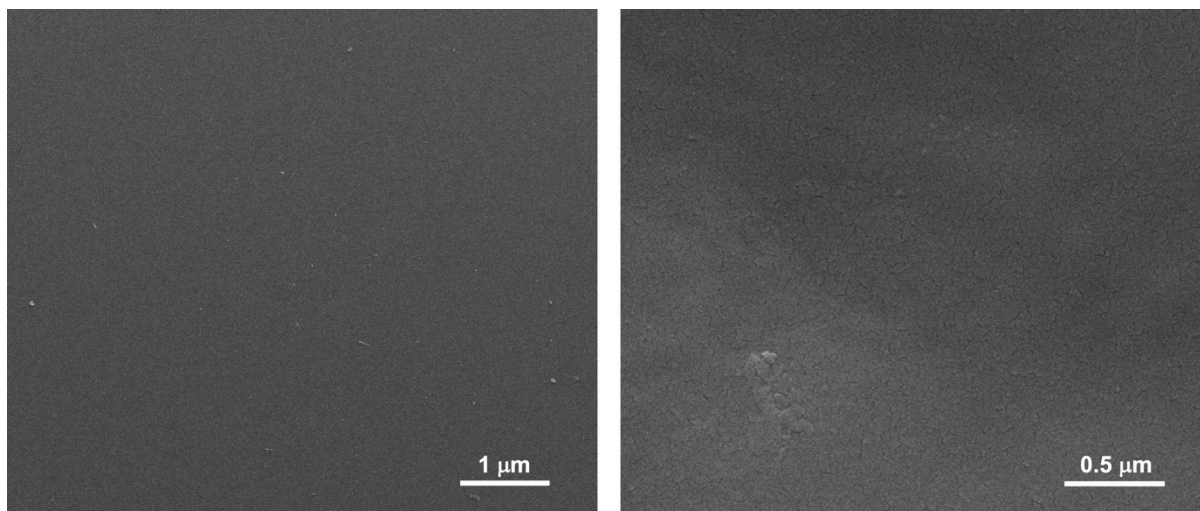


Figure S7. SEM observations after Langmuir-Blodgett transfer on Si at 20 mN/m (left) and 40 mN/m (right) showing the absence of $\text{Gd}(\text{HCOO})_3$ particles.

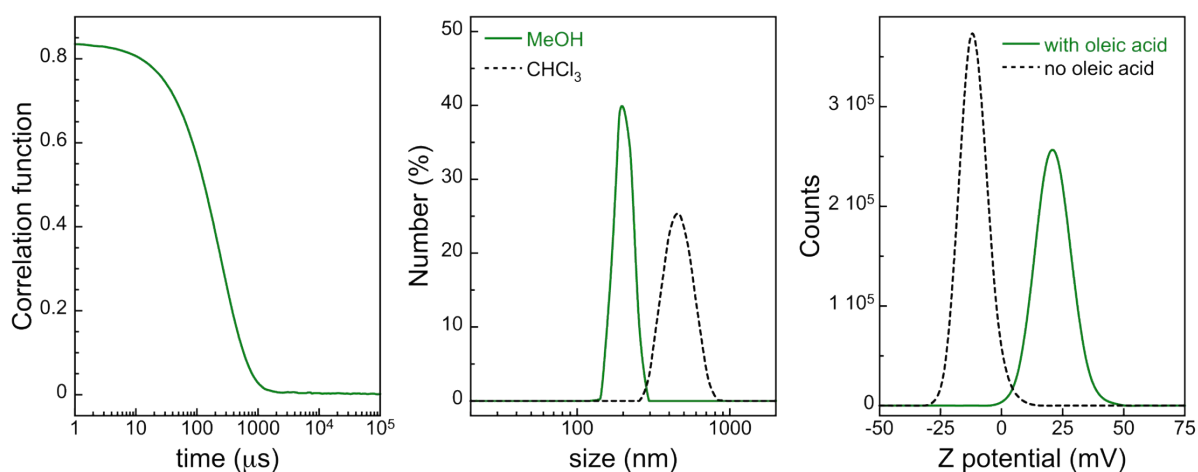


Figure S8. Dynamic Light Scattering of 0.25 mg/mL dispersions of $\text{Gd}(\text{HCOO})_3$ particles coated with oleic acid: correlation function vs. time (left, in MeOH), hydrodynamic size distribution (centre, in MeOH and CHCl_3) and Z potential before and after coating (right).

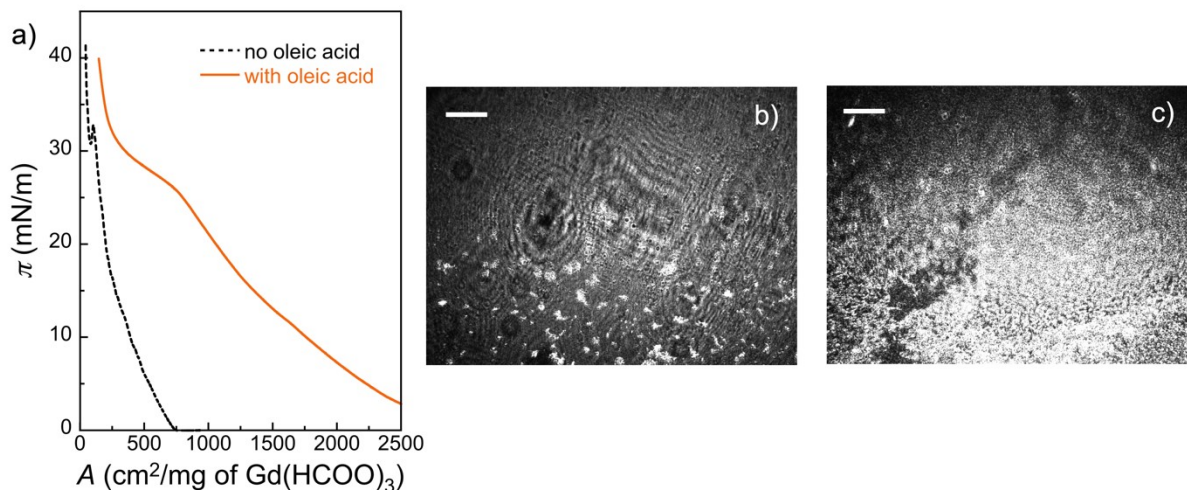


Figure S9. a) Surface pressure-area isotherm for a 0.25 mg/mL dispersion of Gd(HCOO)₃ coated with oleic acid in MeOH:CHCl₃ 1:5 (the isotherm for the uncoated particles is recalled a dashed line for comparison). b) and c) BAM images taken at respectively $\pi = 5$ mN/m 32 and mN/m. The scale bar is 500 μ m.

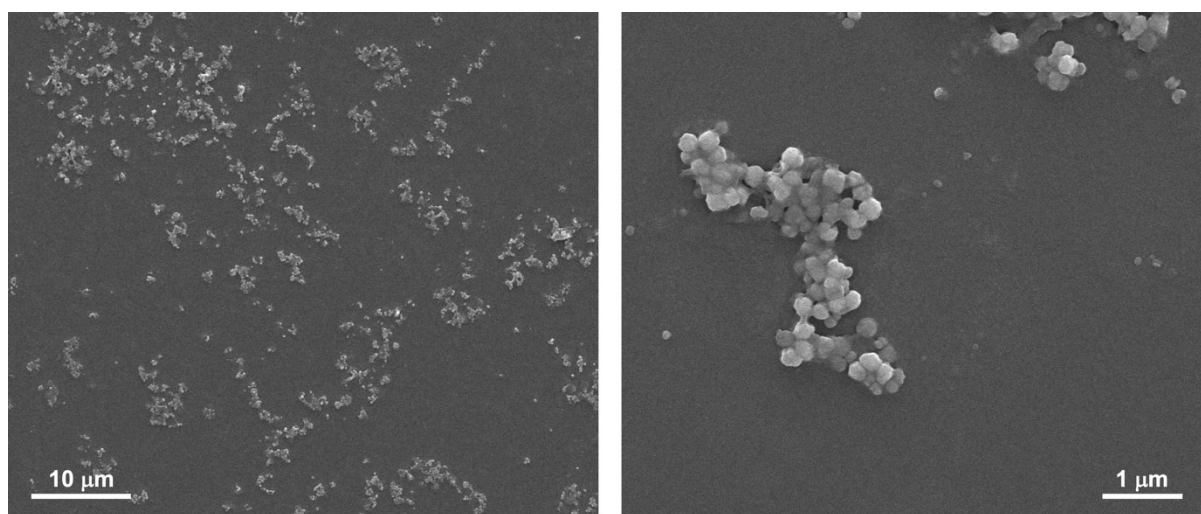


Figure S10. SEM observations at 2 magnifications of the Langmuir-Blodgett film of Gd(HCOO)₃ particles coated with oleic acid transferred on Si at 40 mN/m, showing a very partial and inhomogeneous coverage by groups of particles.

Study of bulk reaction of Gd₂O₃ and formic acid vapors

The formation of Gd(HCOO)₃ by exposing Gd₂O₃ powders to formic acid vapors was studied by placing both reagents, well separated, in hermetic glass vials of either 100 or 200 mL. The reaction was carried out either at 150°C or at 80°C, with variable times and reagent stoichiometry. The combination of the latter and the vial volume allowed to test a range of pressure differences Δp . Two Gd₂O₃ powders, with different grain size, namely > 1 μm and 20-40 nm (though aggregated, see Fig. S12), were tested. Powder diffraction of the recovered solids was used to monitor the completeness of the transformation. A selection of representative patterns is shown in Figure S10.

Initial tests using the larger grain size powder showed that: a) the reaction is less efficient under vacuum and b) more efficient at 80°C. Complete transformation is achieved at 1 atm, 80°C and $\Delta p = 0.78$ atm using stoichiometric conditions.

Further experiments were performed using the smaller grain size powder at 80°C, $\Delta p = 0.65$ atm and stoichiometric conditions. The transformation was found to be complete within 24h at 1 atm and required 48h under vacuum.

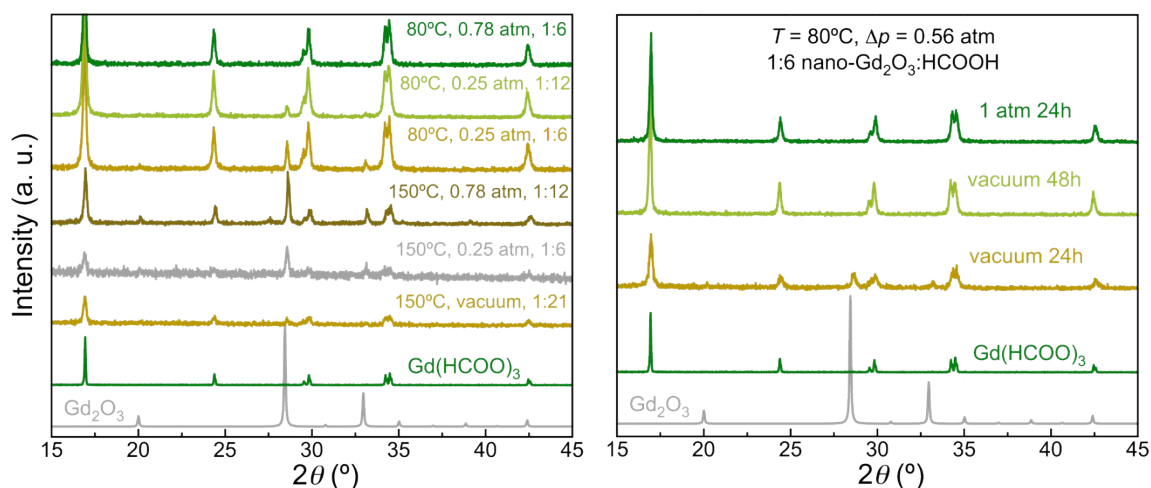


Figure S11. PXR D patterns of the outcome of reactions of Gd₂O₃ powder with formic acid vapors: left) with a > 1 μm grain size powder at the indicated temperatures, Δp and Gd₂O₃:HCOOH stoichiometries, in all cases during 72h; right) with a nano-size grain powder at 80°C and in stoichiometric conditions.

Spin-coating of Gd₂O₃ dispersions

Initial tests to prepare Gd₂O₃ dispersions were made at 0.25 mg/mL, using a commercial nano-powder, supposed to be made of 20-40 nm particles, and different solvents (water, methanol, ethanol and iso-propanol IPA) as dispersants. After 30 min bath ultrasonication, only the dispersion in iso-propanol was visually good and relatively stable.

Dispersions in iso-propanol were thus made additionally at 0.1 and 0.5 mg/mL and characterized by DLS, which showed relatively poor dispersions, with polydispersity indices > 0.45, and large mean hydrodynamic sizes in the range 400-600 nm (Fig. S11). These indicate the presence of aggregates, although SEM observation of the starting powder material shows the used material is, in fact, not nanometric (Fig. S12). Despite the relatively poor quality of the dispersion, initial attempts of spin-coating were made. Static spin-coating systematically resulted in visually inhomogeneous deposits, while dynamic spin-coating seemed to result in continuous films (Fig. S13).

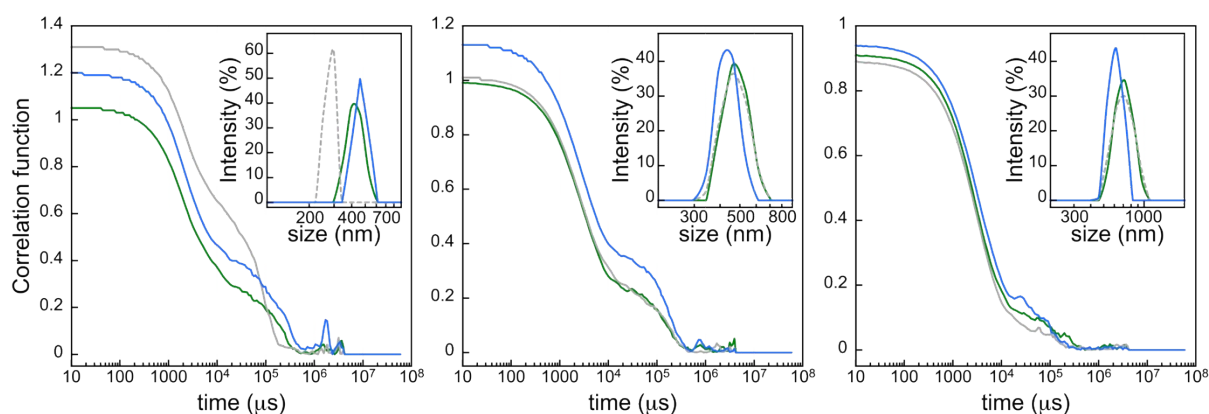


Figure S12. Dynamic Light Scattering dispersions of Gd₂O₃ nano-powder in iso-propanol: correlation function vs. time for 0.1 (left), 0.25 (middle), and 0.5 mg/mL (right) dispersions. The insets show the corresponding hydrodynamic size distribution (by intensity), albeit with poor polydispersity indices of 0.81, 0.75 and 0.48, respectively.

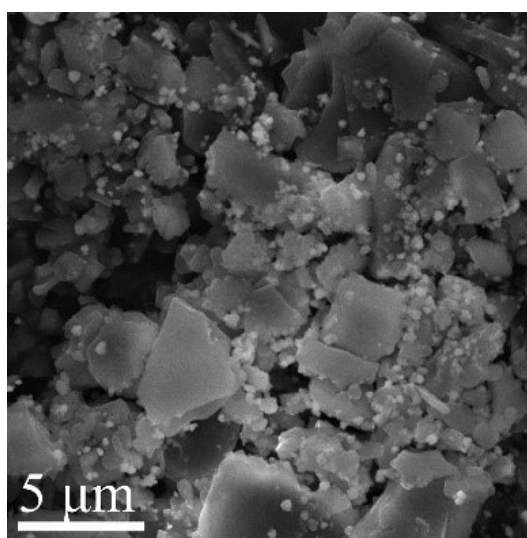


Figure S13. SEM observation of the used Gd₂O₃ "nano"-powder.

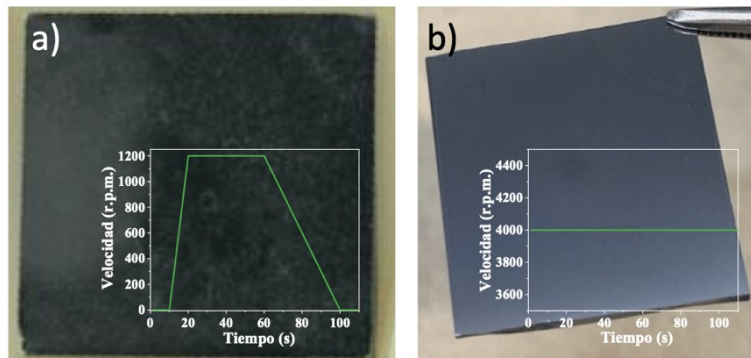


Figure S14. Optical images of the films formed by spin-coating an IPA-Gd₂O₃ dispersion on Si under static (a) and dynamic (b) conditions. The insets show the spinning conditions used. 1 mL of 0.5 mg/mL dispersions was used in both cases.

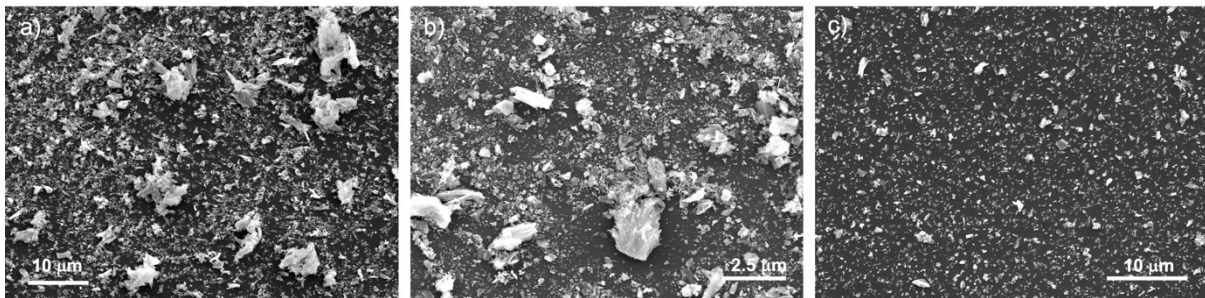


Figure S15. SEM observations of the films obtained by dynamic spin-coating of a 0.5 mg/mL IPA-Gd₂O₃ dispersion on Si under different conditions: a) 4000 RPM 0.25 mL/min during 28 min, b) 4000 RPM 0.5 mL/min during 14 min, c) 6000 RPM 0.5 mL/min during 6 min.

Transformation of Gd_2O_3 films into $\text{Gd}(\text{HCOO})_3$

The reaction was done under the same conditions used for the bulk powder, *i.e.* exposing the films to HCOOH vapors with $\Delta p > 0.6$ atm and $T = 80^\circ\text{C}$, for, respectively, 3 and 24 hours, using an excess of formic acid. GIXRD (Fig. S15) and magnetic (Fig. S16) data show the films are almost fully transformed into $\text{Gd}(\text{HCOO})_3$ after 3h.

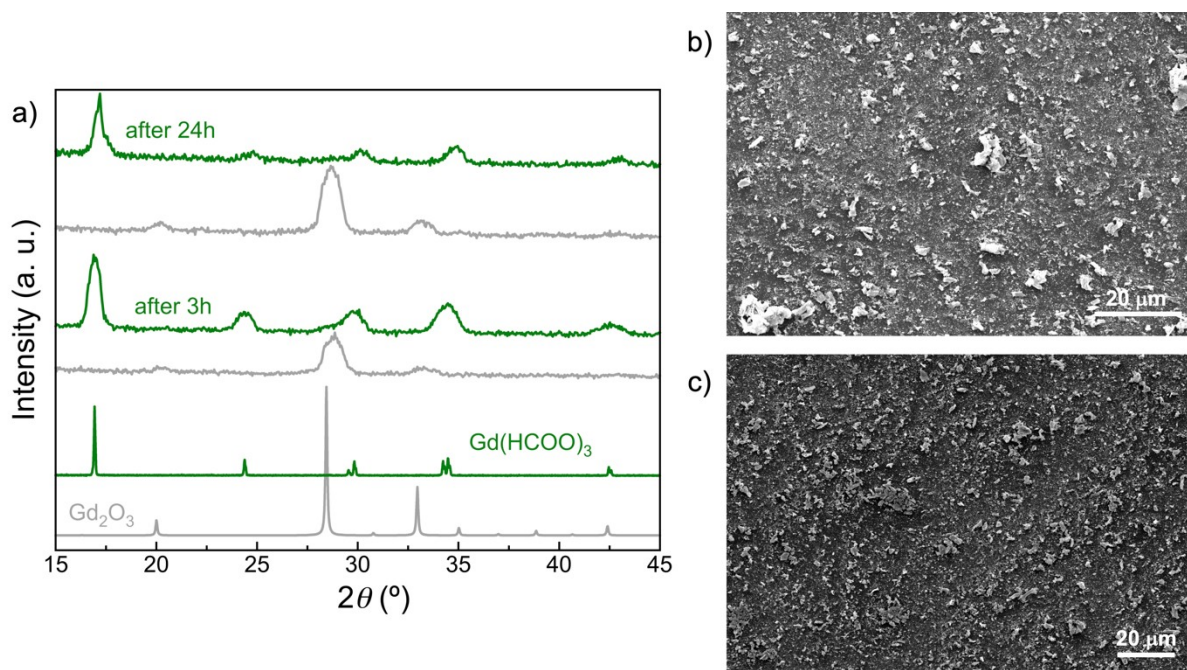


Figure S16. a) GIXRD patterns for spin-coated films of Gd_2O_3 before and after reaction for 3 or 24h, as indicated. b) and c) SEM observations of the films after reaction for 3 and 24h, respectively.

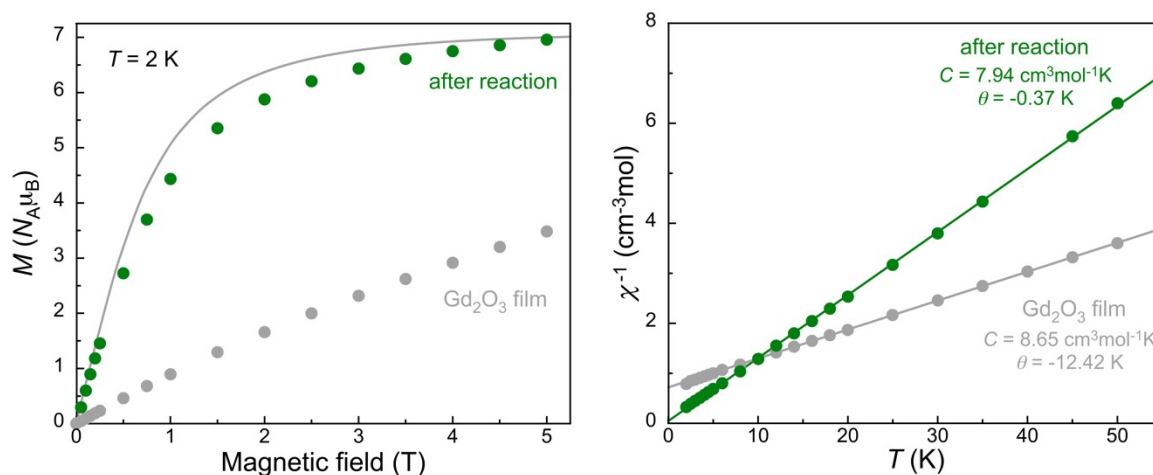


Figure S17. Magnetic characterization of a spin-coated film of Gd_2O_3 before and after reaction for 24h. Left: magnetization vs. field at $T = 2$ K, compared with the Brillouin function for a $S = 7/2$ spin and $g = 2.02$ (grey line). Right: temperature dependence of the inverse scaled magnetic susceptibility χ^{-1} . Lines are fits to the Curie-Weiss law. The slightly higher Weiss temperature θ of -0.37 K after the reaction may indicate the presence of traces of unreacted Gd_2O_3 , that shows a much stronger antiferromagnetic interaction.

Reaction of Gd_2O_3 in formic acid at RT

The reaction of two types of commercial Gd_2O_3 powders (nano-powder, 99.99+% REO and powder, 99.9%, Aldrich, hereafter micro-powder) in formic acid was performed at RT at two concentrations as followed:

- 1) 12.1 mg nano-powder in 24 mL HCOOH
- 2) 13.3 mg micro-powder in 26 mL HCOOH
- 3) 42.9 mg nano-powder in 10.7 mL HCOOH
- 4) 46.0 mg micro-powder in 11.5 mL HCOOH

The four suspensions were subjected to 2×1 hour bath sonication at RT. The solids were recovered by dry extract, resulting in all cases in $\text{Gd}(\text{HCOO})_3$, as shown by PRXD (Fig. S18). The yield was in all cases quantitative. SEM observations indicates the formation of 100-250 nm particles with relatively reduced size dispersion, significantly different from the appearance of the starting Gd_2O_3 powders (Fig. S19).

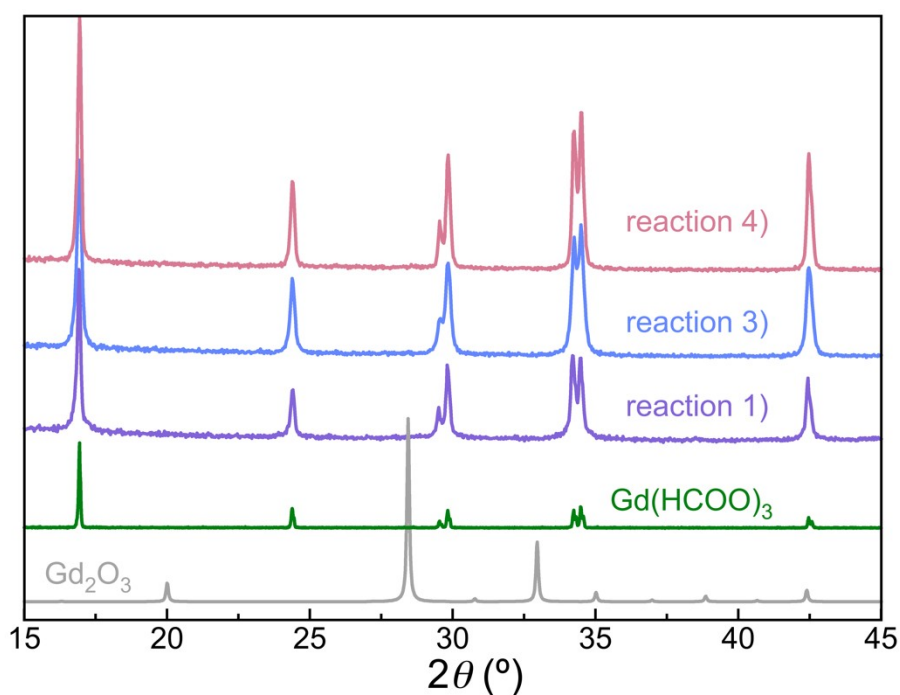


Figure S18. PXRD patterns of the outcome of reactions 1, 3 and 4 above of Gd_2O_3 powders in formic acid at RT under bath sonication.

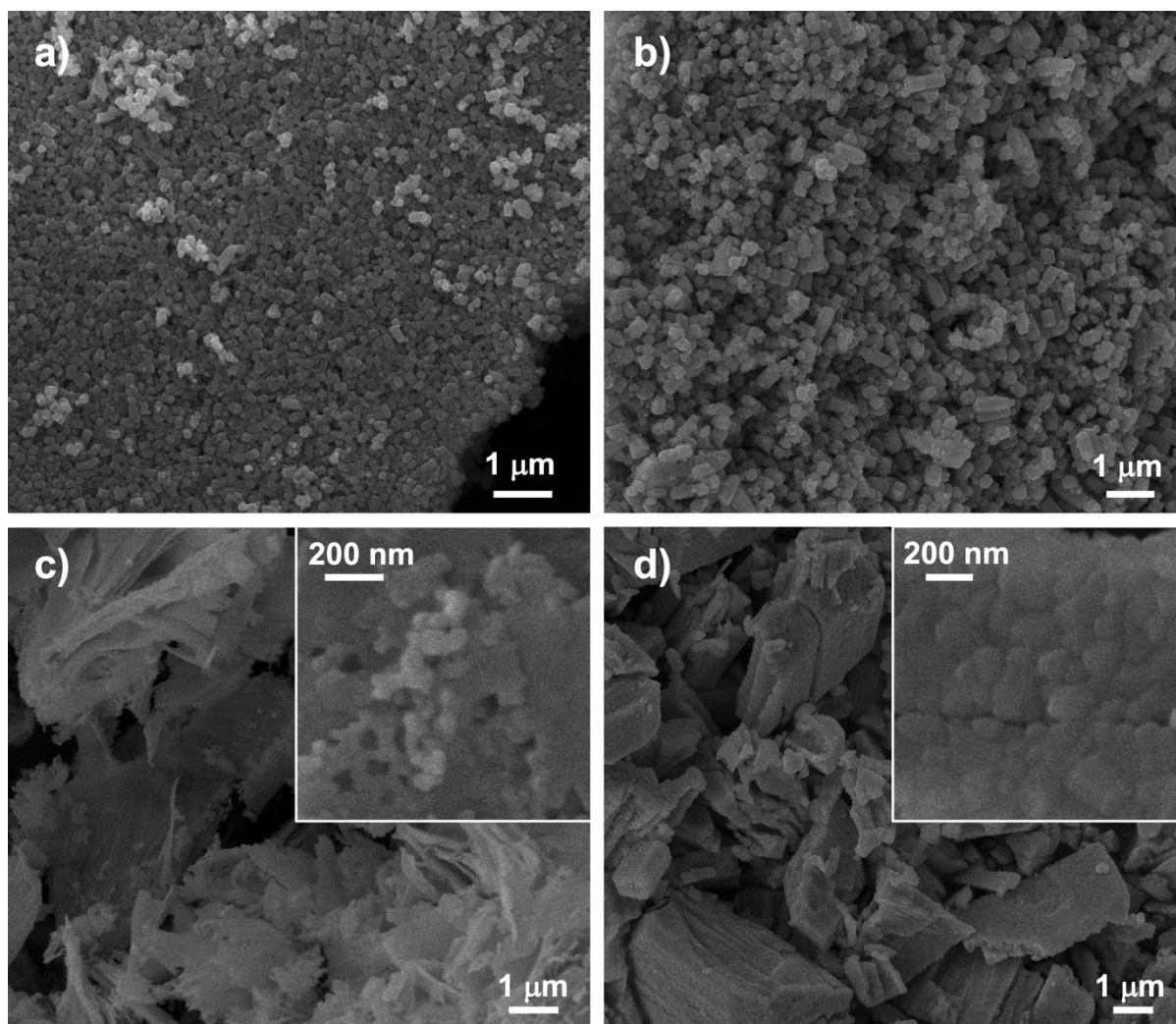


Figure S19. a) and b) representative SEM images of the $\text{Gd}(\text{HCOO})_3$ material recovered from reactions of the “nano” and “micro” Gd_2O_3 powders, respectively. c) and d) representative SEM images at two magnifications of the starting “nano” and “micro” Gd_2O_3 powders, respectively.

Optimization of spin-coating with formic acid dispersions of $\text{Gd}(\text{HCOO})_3$

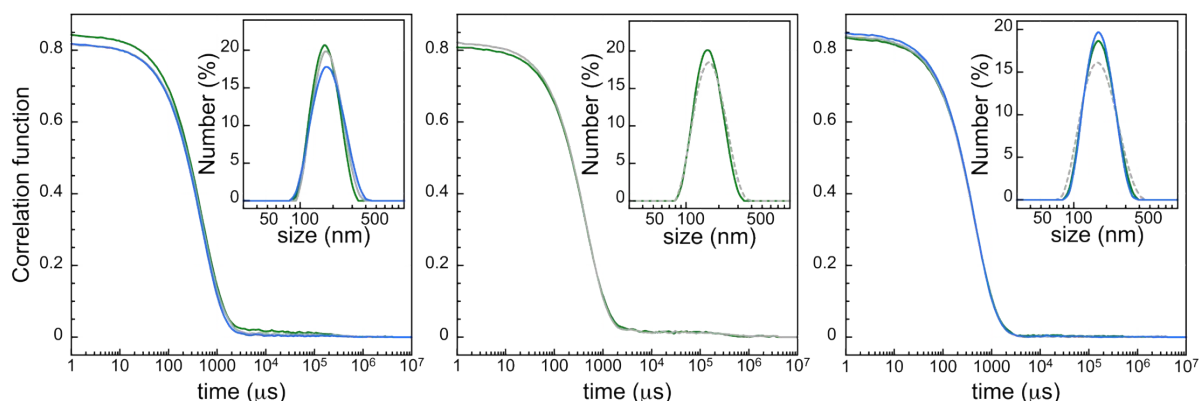


Figure S20. Dynamic Light Scattering of 0.5 mg/mL formic acid dispersions of $\text{Gd}(\text{HCOO})_3$: correlation function vs. time plots for a dispersion freshly prepared (left), 24 hours after preparation (middle) and 7 days after preparation (right). The insets show the corresponding hydrodynamic size distribution (by number), corresponding to 176(45) nm and Pdl= 0.17, 166(44) and Pdl= 0.19 and 165(45) and Pdl= 0.13, respectively.

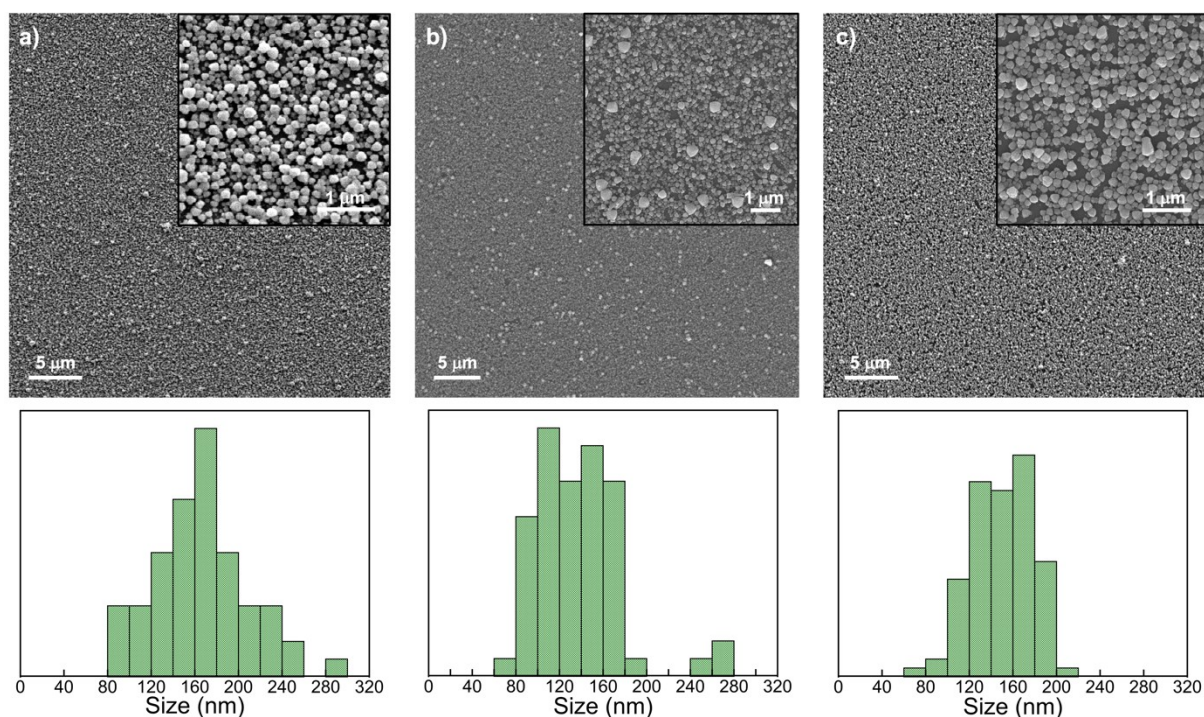


Figure S21. Top: SEM observations at two magnifications of films spin-coated at 4000 RPM and 0.25 mL/min for 21 min, using 0.5 mg/mL dispersions: a) freshly prepared (same day), b) 24h after preparation and c) 7 days after preparation. Bottom: Size distributions derived by analysing images with the program DigitalMicrograph. The mean average sizes are, respectively, 164(43), 140(48) and 150(27) nm.

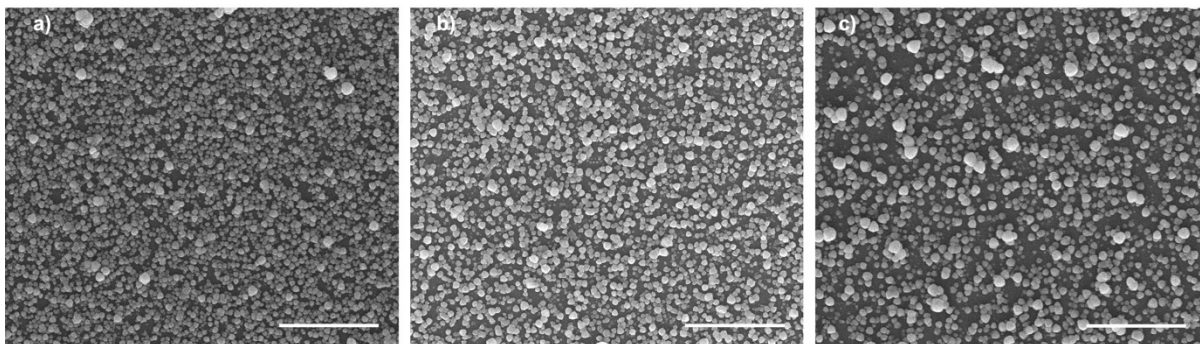


Figure S22. SEM observations of spin-coated films obtained at 4000 RPM by varying only the flux and time during which a 0.5 mg/mL formic acid dispersion is cast: a) 0.25 mL/min over 21 min; b) 0.15 mL/min over 35 min and c) 0.10 mL/min over 45 min. The scale bar is 3 μm in all cases.

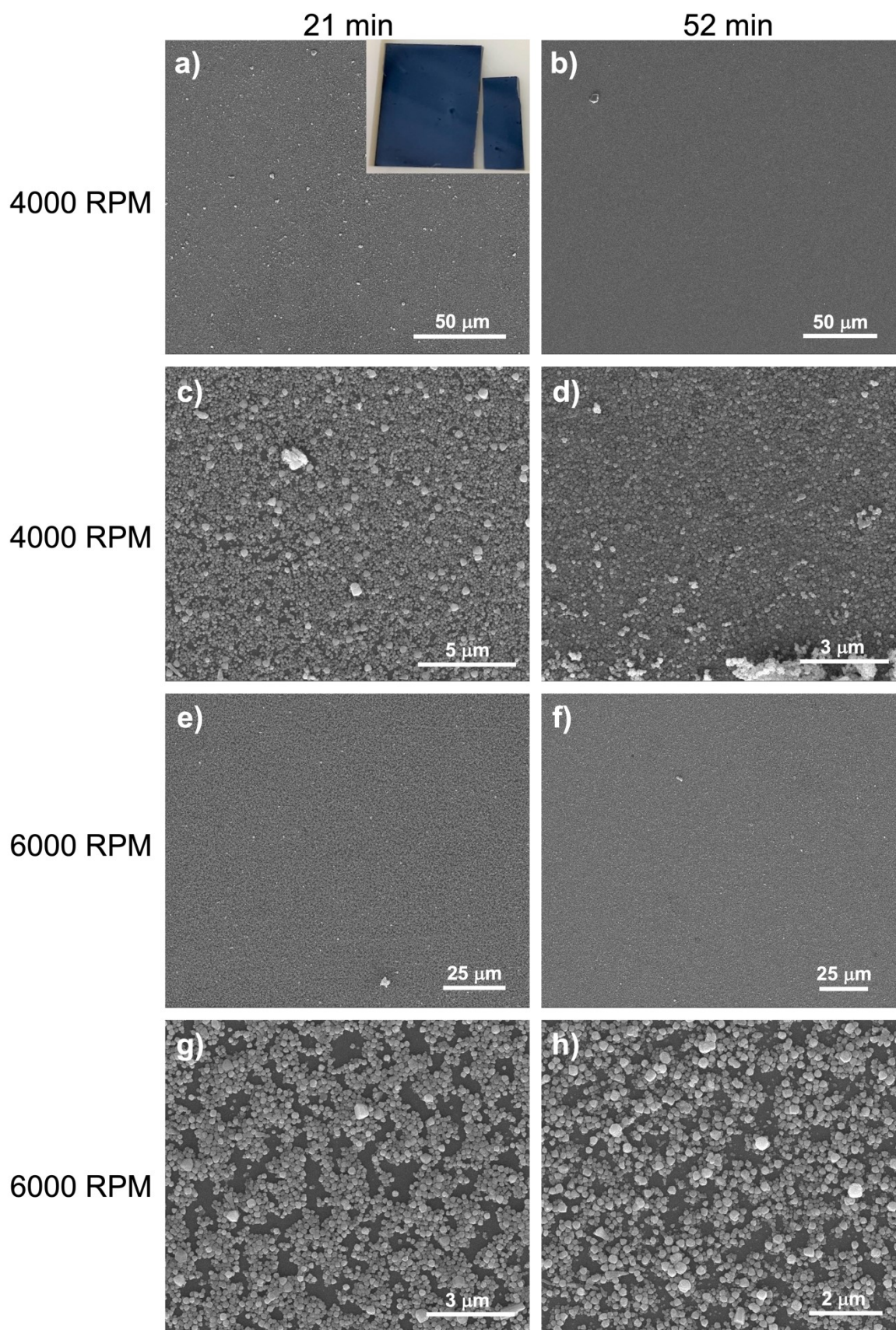


Figure S23. SEM observations of films obtained from 0.5 mg/mL dispersions at either 4000 (a-d) or 6000 RPM (e-g) and for 21 (a-c-e-g) or 52 (b-d-f-g) min at 0.25 mL/min. The inset in a) is an optical picture of the 2×2 cm² Si substrate after cutting it for characterization purposes.

Table S1. Estimation of the surface density of $\text{Gd}(\text{HCOO})_3$ in films spin-coated at 4000 and 6000 RPM using a 0.5 mg/mL dispersion and a 0.25 mL/min flux. The saturation magnetization is taken at $B = 5$ T and $T = 2$ K, using the formula weight 292.3 g/mol. Note the stronger sample to sample deviation for longer spinning time.

Conditions	M_{sat} ($10^{-7} N_{\text{A}} \cdot \mu_{\text{B}} \cdot \text{cm}^{-2}$)	$\langle M_{\text{sat}} \rangle$ ($10^{-7} N_{\text{A}} \cdot \mu_{\text{B}} \cdot \text{cm}^{-2}$)	Mass deposited ($\text{mg} \cdot \text{cm}^{-2}$)
4000 RPM 21 min	7.5	7.0	0.205
	7.6		
	6.0		
4000 RPM 52 min	7.1	11.6	0.339
	15.7		
	5.3		
6000 RPM 21 min	18.4	5.4	0.158
	5.2		
	5.0		
6000 RPM 52 min	6.9	2.9	0.085
	4.3		
	3.3		
	2.4		

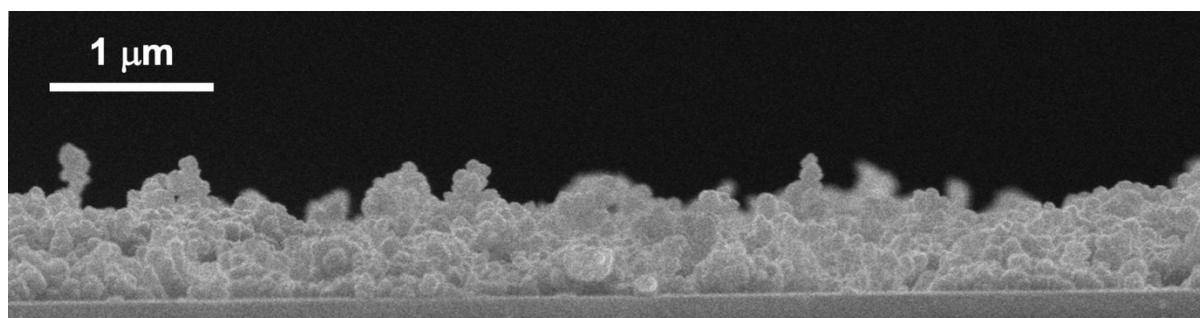


Figure S24. Transverse SEM observation of a spin-coated film obtained with the Si substrate at 50°C. The average height is 0.65 μm .

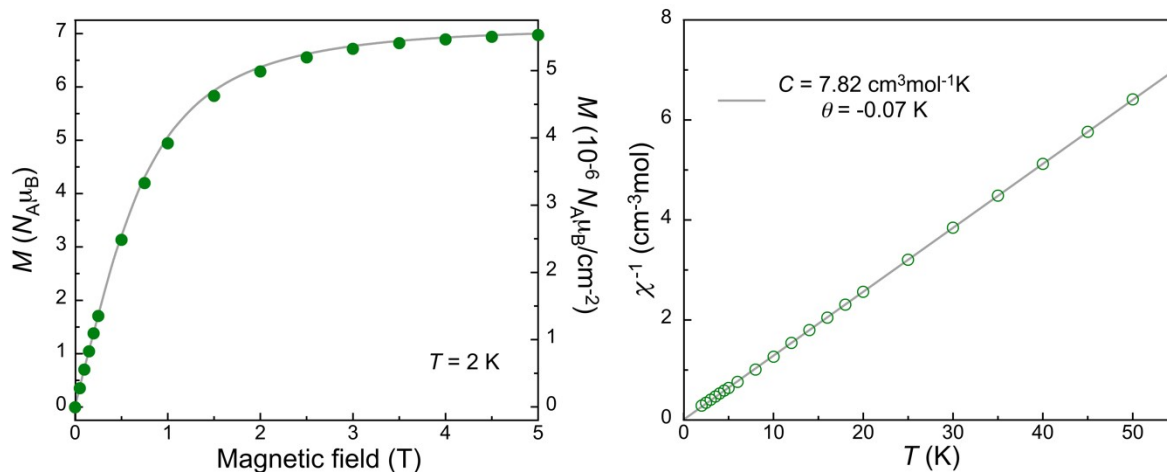


Figure S25. Magnetic characterization of a spin-coated film of $\text{Gd}(\text{HCOO})_3$ obtained with the substrate at 50°C . Left: magnetization vs. field at $T = 2\text{ K}$, compared with the Brillouin function for a $S = 7/2$ spin and $g = 2.02$ (grey line). Right: temperature dependence of the inverse scaled magnetic susceptibility χ^{-1} . The grey line is a fit to the Curie-Weiss law, yielding a Curie constant of $7.82\text{ cm}^3\text{mol}^{-1}\text{K}$ and a Weiss temperature θ of -0.07 K , in excellent agreement with results obtained for the bulk material (see Fig. S2).

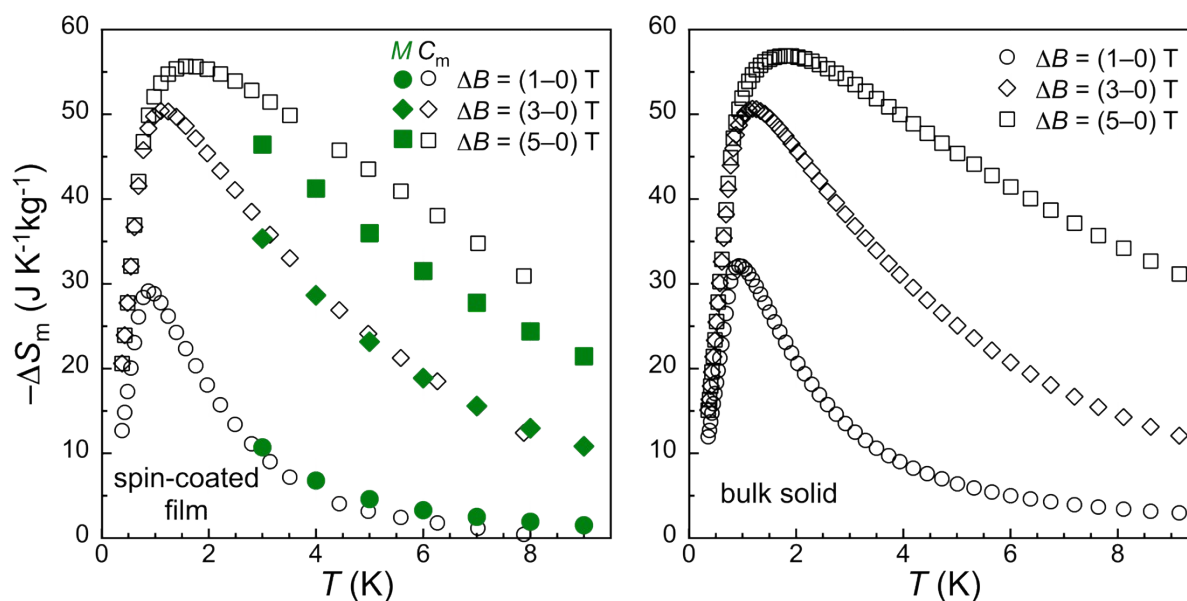


Figure S26. Temperature dependence of ΔS_m for different ΔB expressed in $\text{J K}^{-1}\text{kg}^{-1}$ for spin-coated film of $\text{Gd}(\text{HCOO})_3$, as derived, respectively, from magnetic and calorimetric data, compared with the those previously reported for the bulk material.¹

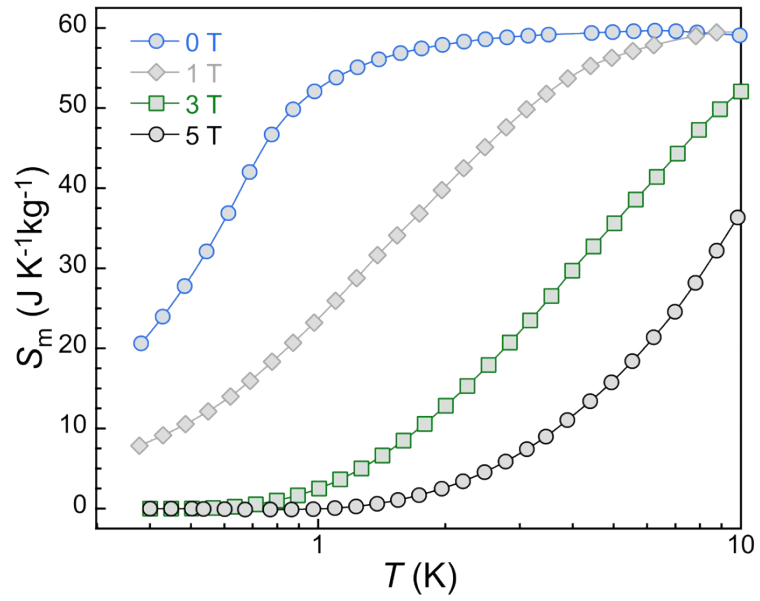


Figure S27. Temperature dependence of S_m for different applied field B for spin-coated film of $\text{Gd}(\text{HCOO})_3$, as derived from integration of $C_m(T)$ data.

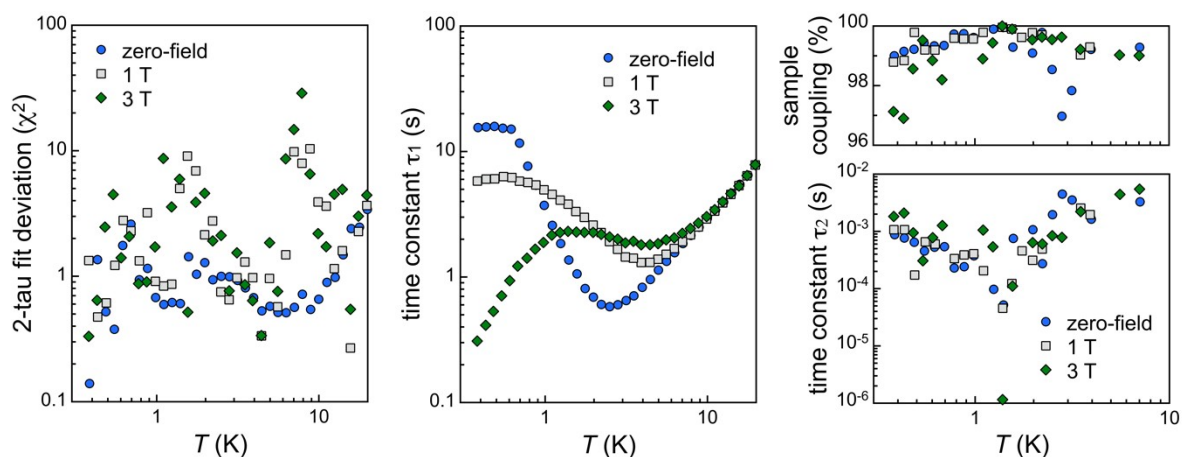


Figure S28: Parameters of the 2-tau determination² of the heat capacity of the whole {sapphire platform + Si + Gd(HCOO)₃ spin-coated film} (see Scheme S1) showing the overall efficient thermal transport at work over the temperature range used for determination of the total entropy S (0.4 – 7 K, Figure 2c of the main manuscript): left, the deviation of the fit of the experimental data to a 2-tau exponential relaxation remains relatively small and similar (χ^2 in the range 0.15 – 10); middle, the main time constant τ_1 depicts the variations in heat capacity and remains in the range 0.3 – 15 s; right, when non-zero the second time constant τ_2 remains very short (< 0.01 s) with a corresponding sample coupling close to 100%.